RESEARCH ARTICLE

https://doi.org/10.21608/fpmpeb.2024.392042

Vol. 1, Issue 3 /No3/2024

Exploring the Toxicological Effects of Silver Nanoparticles: Oxidative Stress and Neurodegenerative Disorders

Eman El Feel[1], Hisham Zaki[2], Hesham Saeed[1]*

[1] Department of Biotechnology, Institute of Graduate Studies and Research, Alexandria University

[2] Department of Environmental Studies, Institute of Graduate Studies and Research, Alexandria University

*Corresponding author: Hesham Saeed, hesham25166@alexu.edu.eg

Abstract

Silver nanoparticles (AgNPs) is used in many industries due to their exclusive antibacterial, antiviral, antiproliferative, and tissue-engineering properties. Toxicological concerns of these nanoparticles was raised due to their accumulation in many organs where they can induce oxidative stress and inflammation. This study aims to study the toxicological effects of AgNPs through biochemical and molecular analysis. Reactive oxygen species (ROS) produced by the presence of AgNPs compromises antioxidant resistance, translocate and cross biological barriers, like the blood- brain barrier (BBB), and accumulate in brain tissues, leading neurodegenerative disorders.

In this study, Wistar male rats were injected intraperitoneally to different doses of AgNPs doses over a three-week period to test both acute and chronic toxicity. Four groups of rats were divided as following: a control group treated with saline and three treatment groups receiving different doses of AgNPs (500 mg/kg for acute, 50 mg/kg, and 30 mg/kg for chronic exposure). Rats' body weights were measured at the end of treatment, blood samples were collected for hematological analysis. Furthermore, the liver and brain tissues were used to examine the presence of AgNPs in cells.

Biochemical tests conducted included measurements of total leukocyte count, erythrocyte count, hemoglobin levels, hematocrit, and red blood cell indices. Liver function tests were conducted along with assessments of antioxidant enzyme activities, such as glutathione S-transferase (GST), glutathione peroxidase (GPx), catalase (CAT), and glutathione (GSH) levels, in addition to evaluating lipid peroxidation through thiobarbituric acid reactive substances (TBARS). In the brain, acetylcholinesterase (AChE) activity and Na^+/K^+ ATPase activity were measured to assess the neurological impacts of AgNP exposure.

The study's results indicate that AgNPs increased oxidative stress markers and induced cellular damage as indication of cytotoxicity. This confirmed the potential toxicological effect of AgNP, especially for nervous system. These findings underscore the further research to determine safe exposure limits the use of AgNPs.

Keywords: Toxicology; Liver; Nanoparticles; Silver.

1. Introduction

Nanotechnology have rapidly developed especially due to new, beneficial properties of nanomaterials. The convergence of nanotechnology with nanomedicine has added new hope in the therapeutic and pharmaceutical field [1]. Decreasing particle size in the nanoscale has been identified as a main parameter for the increased toxicity of nanomaterials. Polystyrene, for

instance, is a very biocompatible polymer used in cell culture however, nanoparticles made from this material are cytotoxic [2].

Silver (Ag) NPs are an example of the numerous different types of NPs being engineered for use in a wide array of consumer, industrial and technological applications [3, 4]. Silver is a metallic element that is utilized in a broad range of applications, such as jewel, cutlery, monetary currency, dental fillings, photography, or explosives [5]. However, silver is better known for its application as an effective antibiotic agent in various products. Recently, it has become popular to use silver in its nanoform into products such as cosmetics, textiles, food boxes, sprays, wound dressings, etc, and today nanoparticles of silver is the most common nanomaterial found in consumer products [6]. Another exposure source is by means of the oral and dermal administration of ionic and nanoparticulate silver as a "universal remedy" [4, 5].

Though AgNPs are used in many antibacterial applications, the action of this metal on microbes is not fully known. It has been hypothesized that silver nanoparticles can cause cell lysis or growth inhibition via various mechanisms. The lethality of silver for bacteria can also be in part explained by thiol group reactions that inactivate enzymes [7]. Silver nanoparticles were found to have an effective bactericidal action against MRSA (Methicillin resistant Staphylococcus aurious) regardless of the resistance mechanisms that confer importance to these bacteria as a drug resistance bacteria [8].

Recent studies of silver nanoparticles as an anticancer agent revealed that exposure of Ag-NPs resulted in chromosomal abnormalities, inhibition of proliferation, observed as failure to form colonies, and absence of recovery selectively in cancer cells, which add new hopes for preventing cancer cell metastasis [9].

Studies on bio-distribution of AgNPs administered to rats orally or intravenous injection indicate that the highest absorption occurs in liver, spleen, kidney, and gonads, with the lowest observed in lungs and brain [10, 11]. When these nanoparticles administered via intranasal or inhalation routes, silver concentrations were enhanced in blood, liver, lungs, kidney, olfactory bulb, and brain [12].

Based on the previous studies, it can be revealed that AgNPs enter the brain via the upper respiratory tract and mobilize along nerves in the olfactory bulb when administered by inhalation, or via the BBB when administered systemically or orally. In addition, it was found that the brain is not cleared of accumulated AgNPs, even during a prolonged recovery period. AgNPs of small diameter have a long half-life in the brain, indicating that the BBB impedes their transfer back to the blood. The tendency of AgNPs to accumulate in the brain increase the risk of significant long-lasting pathological effects [13].

Recent literature suggests cytotoxicity to be related to oxidative stress and pro-inflammatory gene activation [14]. Further to particle-related factors, the administered dose, route of administration and extent of tissue distribution seem to be important parameters in nano-toxicity. Typically, cell-based toxicity studies use increasing doses of the NP in order to observe dose-related cellular or tissue toxicity. Such dose response correlations are the basis for determining safe limits of particle concentrations for in vivo administration. It is sensible to assume that bio-distribution, accumulation, metabolism and excretion of NPs will differ depending on the route of administration as will its toxicity. Different routes of administration show different rates of distribution and accumulation thus this shows different rates of toxicity [15]. Pulmonary exposure shows tremendous potential toxicity due to NPs aggregation and subsequent tissue inflammatory reactions. Intravenous and oral NPs administrations inherently have a more rapid systemic effect compared to transdermal administration and once within the circulation, most substances are subject to first-pass metabolism within the liver where they may accumulate or distribute via the vasculature to end organs including the brain. Despite its innate protection by the BBB against external chemical insults, the potential for nanoparticulate matter to percolate through tight junctions renders the brain vulnerable to potential particle-mediated toxicity [16]. Topically applicable nanoparticles show potential local toxicity with mild systemic effects depending on frequency and dose to be applied. Topically and systemic ingested silver nanoparticles can induce the benign condition known as argyria, a grey blue discoloration of the skin and liver caused by deposition of Ag particles in the basal laminae of such tissues. This has prompted a limitation on the recommended daily dosage of Ag [17]. Furthermore, numerous toxicity studies focusing on AgNPs have been carried out on cell lines including mouse fibroblast, rat liver, human hepatocellular carcinoma and human skin carcinoma cells showing a potential rise in ROS and oxidative-stress mediated cell death and apoptosis [18]. Dermal penetration studies are ideally carried out on porcine skin due to its resemblance to that of humans in terms of thickness and rate of absorption. Many studies have indicated the propensity for AgNP to accumulate within the liver and induce oxidative stress-related toxicity. Certain parameters influencing the degree of toxicity include particle concentration, size, shape and the ability to deplete

cells of antioxidants [19].

Oxidative stress-dependent cytotoxicity was firstlay confirmed by Kim *et al*., 2009 who were able to significantly improve viability of rat hepatoma cells exposed to AgNP after pre-treating cells with the naturally occurring anti-oxidant N-acetylcysteine [20].

A study conducted by Costa *et al*., suggests mitochondrial dysfunction and impaired energy production as the possible underlying mechanism of neurodegeneration [21]. AgNPs results in a reduction in synaptic proteins, cytoskeletal integrity, mitochondria functionality and cell viability in a dose-dependent manner [22]. Specifically, AgNPs not only inhibited neurite extension and overlap during the early stage of neuronal development, but also caused degeneration of neuritic processes or aberrant aggregations of cell bodies in well-established neurons and their networks. AgNPs-induced neurotoxicity involved altering cytoskeletal proteins (e.g.β-tubulin and F-actin), dissolution of synaptic proteins and compromising of mitochondria function [23, 24].

The aim of this study was to investigate the effects of silver nanoparticles (AgNPs) on biochemical and molecular parameters in rats, with a particular focus on elucidating the potential link between AgNP toxicity and the incidence of neurodegenerative diseases. Furthermore, by examining AgNP-induced oxidative stress, inflammation, enzyme inhibition, and their potential elevation. Through this research, we intend to elucidate the link between AgNP toxicity and neurodegeneration.

2. Materials and Methods

All chemicals used were of either analytical reagent, molecular biology or chromatographic grade as appropriate. Silver nanoparticles (Ag nps) were obtained from Nanomaterials Co., USA. Spherical silver nanoparticles with a mean diameter of 20nm were used throughout the experiment.

The physical properties of silver nanoparticles were characterized using Scanning Electron Microscope, Electron Microscope Unit, College of Science, Alexandria University, Alexandria, Egypt.

2.1 Animals and Treatments

Male rats weighing approximately 140- 160 g were obtained from Egyptian Company for Serums, Vaccines and Medicines, Helwan, Cairo, Egypt. The animals were housed in cages (6 per cage) in the animal house facilities at the Inistitute of Graduate Studies and Research, Alexandria University. The animals fed a standard laboratory diet and water. The animals were kept under controlled hygienic conditions and maintained at a temperature 24 $\pm$ 1°C with 50% humidity and time controlled lighting to a 12 h light/day. Rats were kept for two weeks for acclimation at room temperature before treatment. All rats were handled in accordance with the standard guide for care and use of laboratory animals (OECD 1992 guidelines 407). The rats were divided into four groups 6 animals each. A control group, received normal saline at dose of 1 ml/rat intraperitoneal three times per week. Silver nanoparticles acute dose group were received a single dose of 500 mg/kg body weight of SNPs intraperitoneal. Silver nanoparticles were prepared in deionized water and solubilized by sonication at room temperature for 30 minutes. A third group, silver nanoparticles high does chronic group were received 50 mg/kg body weight of SNPs intraperitoneal for three times per week and for three weeks. The fourth group, silver nanoparticles low dose chronic group were received 30 mg/kg body weight of SNPs intraperitoneal for three times per week and for three weeks.

The concentration of silver nanoparticles used in this study was determined from sub lethal dose according to LD50 of silver nanoparticles mentioned in material safety data sheet and literature reviews. AgNPs were dissolved in deionized water and by sonication. After treatment, the animals were sacrificed after being anesthetized with light ether. Liver and brain tissues were rapidly removed from the animal groups and placed on ice. Small fractions from the brain tissues were removed immediately and immersed in RNA Later solution (Ambion, Courtier, France) and kept at 4 °C for overnight after which all samples are stored at -20 °C till used for RNA isolation and purification. Blood samples were also collected by direct heart puncture in heparin treated sterilized tubes.

2.2 Total protein Determination by Lowry

Total protein was determined according to Lowry [25]. For each protein sample to be determined, 2.5 ml of reagent E was added, mixed well and let to stand for 10 minutes at room temperature. After which, 0.25 ml of reagent F was added and mixed well and let to stand for 30 minutes at room temperature then, the absorbance was measured at 750 nm against a blank of 0.5 ml of sample buffer containing the same reagents previously described and under identical assay conditions. Bovine serum albumin (Sigma- Aldrich chemical Co, USA) was used as a standard at a concentration of 0.5 mg/ml.

2.3 Biochemical Characteristics of Blood

Blood samples collected in heparin-treated tubes were analyzed for hematological parameters Hb, hematocrite, packed cell volume (PCV), Red Blood Cells (RBCs) count and White Blood Cells (WBCs) count. Plasma was collected by centrifugation at 700xg for 20 minutes and stored at -80 °C.

Hemoglobin concentration was measured in the whole blood shortly after collection using Hb determination kit (Diamond Diagnostics Egypt). RBCs were counted on an AO bright line hemocytometer using a light microscope at 430 X magnification. Blood samples were diluted 200 times with physiological saline solution before counting. Microhematocrit tubes with a hematocrit centrifuge at a speed of 16,500 xg for 5 minutes were used to determine PCV. WBCs were counted on AO bright line hemocytometer using a light microscope at 100 X magnification after diluting blood samples 20 times with a diluting fluid containing, 1% acetic acid and a few microliters of Leshman's stain before counting.

Blood indices were calculated according to Wintrobe *et al*., [27] to determine the changes in red blood corpusles as follow; MCV (cu μ) = PCV (%) No. RBCs per 100 ml, MCH (pg) = Hb (gm per 100 ml)/ No. RBCs per 100 ml, and MCHC (%) = [Hb (gm per 100 ml)/PCV (%) x 100.

2.4 Measurement of Liver function

2.4.1 Assay of Aspartate Aminotransferase (AST)

AST was measured according to Reitman and Frankel (1957) [27]. The incubation reaction contained 0.5 ml of AST substrate (0.1 M phosphate buffer pH 7.5, 0.002 M α-oxoglutarate and 0.2 M L-aspartic acid). The protein samples 0.1 ml were then added and the reactions were proceeded at 37°C for 60 minutes. Color forming reagent, 2,4-dinitrophenylhydrazine, was then added and the reactions tubes were left for 20 minutes at room temperature after which the alkaline reagent, 0.4 N NaOH was then added and left for 5 minutes. The absorbance was read at 505 nm against a blank solution containing distilled water.

2.4.2 Assay of Alanine Aminotransferase (ALT)

ALT was measured according to Reitman and Frankel [27]. The reaction mixture contained 0.5 ml of ALT substrate (0.1 M phosphate buffer pH 7.5, 0.002 M α-oxoglutarate and 0.2 M dL-alanine). The mixture was incubated at 37 °C for 5 minutes followed by the addition of 0.1 ml of sample after which the reaction was continued for 60 minutes at 37 °C. Color forming reagent (2,4-dinitrophenylhydrazine) was then added and left for 20 minutes at room temperature after which alkaline reagent 0.4 N NaOH was added and left for additional 5 minutes. The absorbance was read at 505 nm against blank solution containing distilled water.

2.4.3 Assay of Alkaline Phosphatase (ALP)

ALP was measured according to Belfield and Goldberg [28]. Reaction mixture contained 0.5 ml of 50 mM phosphate buffer, pH 10.0 and 5 mM phenylphosphate and 0.025 ml of protein samples. The reaction mixture was incubated at 37 °C for 20 minutes after which the reaction was terminated by the addition of 100 mM EDTA and 50 mM 4-aminophenazone. Color forming reagent composed of 200 mM potassium ferricyanide was then added to the reaction tube, mixed well and stand for 5 minutes at room temperature in dark place. The liberated ρ-nitrophenol was then measured spectrophotometrically. One ml of working reagent, 10 ml of buffering reagent contained, 0.9 M/L 1-amino-2-methyl-1-propanol buffer pH 10.5 and 2 mM magnesium sulfate to substrate reagent,
5.5 M ρ-nitrophenylphosphate. This mixture was incubated at 37 °C for 30 minutes after which the alkaline reagent, 10 ml of 0.4 N NaOH was then added and the absorbance was read at 510 nm. One unit of enzyme activity was the amount of enzyme that liberate one micromole of phenol per minute at the indicated temperature.

2.5 Measurement of Brain Toxicological effects

2.5.1 Assay of Acetylcholinesterase (AChE)

Assay of Acetylcholinesterase (AChE) in the brain

Brain tissue was homogenized in a glass Teflon homogenizer in a buffer solution contained 0.25 M sucrose, 1% Triton-X100 in 0.1 M phosphate buffer pH 7.4 in a ratio of 1:3 (brain tissue weight: buffer). After homogenization, filtration was carried out through double sheath cloth after which centrifugation was done at 10,000 xg for 10 minutes. The supernatant was collected, aliquots and stored at -80 °C until it used for acetylcholinesterase assay.

Acetylcholiesterase activity was measured according to Ellman *et al*., [29]. The reaction mixture contained 750 µl of 0.1 M phosphate buffer pH 7.4, 25 µl DNTB and 100 µl brain tissue homogenate. The reaction tubes were then shaken and the absorbance of the yellow color produced was measured spectrophotometrically at 412 nm previously adjusted to zero using a blank contained all of the reagent mix except the enzyme. 25 µl of 0.075 M acetylcholine iodide was added gently to ensure thoroughly mixing and the absorbance was measured every 30 seconds over a period of 7 minutes. Specific activity was expressed as µmoles product formed per minute per mg protein using molar extinction coefficient of the adduct formed between thiocholine and DTNBas 13.6 μM^{-1} cm^{-1}.

2.5.2 Assay of Adenosine Triphosphatase (ATPase)

Isolation of mitochondria from the brain tissue, Brain tissues were dissected and placed on ice cold medium containing 0.25 M sucrose, 1 mM EDTA, and 20 mM Tris-HCl, pH 7.4 and homogenized with Teflon homogenizer for 30 seconds. The brain

homogenate was filtered through a double layer of cheese cloth after which centrifugation was carried out at 750 xg for 10 minutes at 4 °C using high speed centrifuge Beckman Model J 2-21. The supernatant fraction was the collected and centrifuged at 9000 xg for 10 minutes at 4 °C to give a mitochondrial pellet. Mitochondrial pellet was resuspended in 0.25 M sucrose and stored at -20 °C until used for the assay.

2.5.3 Assay of Mitochondrial brain Na^+/K^+ ATPase

Brain mitochondrial Na^+/K^+ ATPase activity was determined using end point of phosphate analysis following the method of Taussky and Shorr [31]. A 1.0 ml reaction mixture contained 5 mM ATP, 5 mM $MgCl_2$, 100 mM NaCl, 20 mM KCl, 135 mM imidazole/HCl buffer, pH 7.5 and 35-40 µg of enzyme. The reaction was initiated by the addition of the mitochondrial fraction and allowed to proceed for 30 minutes with constant shaking at 37 °C. After the incubation period the reaction was terminated by the addition of 0.1 ml of 50% ice-cold TCA. The total ATPase activity was measured in the presence of Na^+, K^+, and Mg^{+2} ions in the reaction mixture. The Mg^{+2} ATPase was measured in the presence of 1 mM oubain, a specific inhibitor for Na^+/ K^+ ATPase. Na^+/ K^+ ATPase was determined as the difference between total and Mg^{+2} ATPase. Inorganic phosphate was estimated in each supernatant fraction and the absorbance obtained was compared to a standard curve of known Na_2HPO_4 concentrations between 0.1-1 µmoles/ml.

2.6 Determination of antioxidant enzymes

2.6.1 Determination of Glutathione S-transferase (GST)

Glutathione S-transferase activity in the liver homogenate was measured according to the method of Habig *et al*., [32]. The reaction mixture contained 30 µg protein of the supernatant fraction, 0.5 ml reduced glutathione (0.5 mM), 0.1 ml sodium phosphate buffer pH 7.3. Preincubation was carried out for 5 minutes at 37 °C followed by the addition of 50 µl of 1-chloro-2,4-dinitrobenzene (CDNB, 0.5 mM) and incubation was continued for 5 minutes at 37 °C. The reaction was terminated by the addition of 0.2 ml of 33% TCA. Centrifugation was carried out for 5 minutes at 3000 rpm and CDNB conjugate was measured spectrophotometrically at 340 nm.

2.6.2 Measurement of Reduced Glutathione

Reduced glutathione was measured in rat liver homogenate according to Beutler *et al*., [33] utilizing a commercial kit obtained from Biodiagnostics Co., Egypt. The reaction was done by adding 0.5ml of liver homogenate with 0.5ml TCA, mixed and centrifuged at 3000rpm for 15min. 0.5ml of supernatant was added to 0.1ml DTNB in 0.5ml reaction buffer, mixed well and the absorbance was measured at 405 nm. The reduced chromogen is directly proportional to GSH concentration at 405 nm.

2.6.3 Assay of Catalase

Catalase was measure in rat liver homogenate according to Aebi *et al*., and Fossati *et al*., [34, 35] utilizing a commercial kit obtained from Biodiagnostics Co., Egypt. One unit of catalase is the amount of enzyme that decomposes 1 µM of H_2O_2/minute at 25 °C and pH 7.0. Catalase reacted with a known concentration of H_2O_2 for one minute after which the reaction was terminated by the addition of catalase inhibitor. In the presence of horse radish peroxidase (HRP), the remaining H_2O_2 reacted with 3,5-dichloro-2-hydroxybenzene sulfonic acid (DHBS) and 4-aminophenazone (AAP) to form a chromophore with color intensity inversely proportional to the amount of catalase present in the original sample.

2.6.4 Assay of Glutathione Peroxidase

Glutathione peroxidase activity (GPx) was measured according to Paglia and Valentine (1967) [36] utilizing a commercial kit obtained from Biodiagnostics, Egypt. The oxidation of NADPH to $NADP^+$ is accompanied by a decrease in absorbance at 340 nm providing a spectrophotometric means for monitoring GPx enzyme activity. The reaction mixture containing 1 ml 50 mM phosphate buffer, Triton-X100, pH 7.0), 0.1 ml NADPH 24 µM and 0.01 ml of the liver homogenate. The reaction is started by the addition of 0.01 ml diluted hydrogen peroxide and the decrease in the absorbance was recorded at 340 nm over a period of 3 minutes. Enzyme activity was determined using a molar extinction coefficient of NADPH 6220 M^{-1} cm^{-1}. The rate of decrease in the absorbance is directly proportional to the GPx activity in the sample.

2.6.5 Measurement of Thiobarbituric acid reactive substances (TBARS)

Thiobarbituric acid reactive substances were measured as described by Tappel and Zalkin (1959) [37]. One ml of homogenate was added to 2ml of 7.5% trichloroacetic acid and mixed well after which centrifugation was carried out at 1000 xg for 10 minutes and 2ml of the supernatant was added to 1ml of 0.7% 2-thiobarbituric acid. After boiling for 10 minutes the reactants were cooled and TBARS were measured at 532 nm. As extinction coefficient of 156,000 $M^{-1}cm^{-1}$ was used for calculations.

2.7 RNA Extraction and Quantitative polymerase chain reaction

Frozen reserved brain tissues were retrieved from the RNA later solution and left on ice to completely be thawed. Brain tissue samples, 60 mg each, were

then homogenized in RNA lysis solution. The total RNA was prepared using PREP-NA-S DNA/RNA Extraction Kit "DNA-Technology Research & Production", LLC, 142281, Russia, Moscow Region" in line with the instructions obtained from the manufacturer. The quantity of the extracted RNA was confirmed by Nanodrop Sambrook *et al*., 1989 [38]. Next, complementary DNA (cDNA) was synthesized using a SensiFAST™ cDNA synthesis kit (Bioline/Meridian Bioscience, London, UK) in line with the manufacturer's instructions. The cDNA samples were then stored at −20 °C until use. Quantitative real-time PCR analyses were carried out using the SYBR premix Ex Taq 2 kit (Takara) in a final volume of 25 µl with 10 pmol of each primer by the CFX96 real-time PCR detection system (BioRad, USA). Each assay was run in the triplicate manner with each set of primers [39].

All primers under study and the prepared cDNA were tested for amplification specificity using simple PCR in an attempt to adjust the conditions for measurement of the level of gene expression for all genes by real time PCR. PCR was carried out in 50 µl final volume contained 5 µl of cDNA, 3 µl (30 pmole) of each forward and reverse primer, 25 µl of 2x PCR master mix and 17 µl nuclease free water. PCR conditions for each primer and the expected products sizes are as following β-actine primers FWD 5'- TAC AAC CTC CTT GCA GCT CC -3', REV 5'- GGA TCT TCA TGA GGT AGT CAG TC -3' the expected product size is 425bp, PCR program is set as following; 5min at 95ºC (1x)30 sec at 95ºC (40 x) and 45sec at 58ºC (40 x), Tyrosine Hydroxylase (TH)**;** FWD 5'TACCTCCGGGTGACAGCATA -3', REV 5'GGGCTGTGGAGACAGAACTC -3' the expected size is 120 bp, PCR program is set to 5 min at 95ºC (1x), 30 sec at 95ºC (40 x) 45sec at 58ºC (40 x), Monocyte Chemoattractant Protien (MCP)**,** FWD 5' CTGTAGCATCCACGTGCTGT -3'**,** REV 5'GGTGCTGAAGTCCTTAGGGT -3' the expected size is 290 bp PCR program is set to 5 min at 95ºC (1x), 30 sec at 95ºC (40 x) 45sec at 55ºC (40 x), Vesicular Monoamine Transferase (VMT) FWD 5'TCACTGTGGTGGTGTTTGCT-3', REV 5'-ATTCCCATGGCTCTCCCTCT -3' the expected size is 156 bp PCR program is set to 5min at 95ºC (1x), 30 sec at 95ºC (40 x) 45sec at 55ºC (40 x), Inducible Nitric Oxide Synthase (iNOS); FWD5'GCCCAACAACACAGGATGAC-3' , REV5'CCTTGTGGTGAAGGGTGTCG-3' the expected size is 191 bp PCR program is set to 5min at 95ºC (1x), 30 sec at 95ºC (40x) and 45 sec at 58ºC (40x).

The real time PCR conditions were as followed, initial denaturation at 95 °C for 5 minutes followed by 40 cycles for 30 seconds at 95 °C, annealing and elongation for 1 minute at 60 to 65 °C according to the primers melting temperature one cycle at 95 °C for 1 minute. After the end of the run CT values (threshold cycle value) were analyzed manually at a factor of 0.04. Amplification and melting curves and CT values were collected for statistical analysis of the results. The expression of targeted genes was normalized to the reference gene β-actin expression levels within the same sample to determine ΔCT. This step serves to correct for non-treatment-related variation among wells such as potential differences in cell number. ΔCT was then normalized to the expression of the targeted gene in treated animals from a separate untreated sample to find ΔΔCT. % Expression was calculated by the equation (%Expression = $2^{-\Delta\Delta CT}$).

2.8 Statistical analysis

The data were analyzed using Graph Pad Prizm7 2016. The significance of the differences was calculated using one-way ANOVA followed by Dunnett's test for multiple comparisons. $P < 0.05$ was considered statistically significant.

3. Results and Discussion

3.1 Characterization of Silver Nanoparticles using Scanning Electron Microscope

The scanning electron micrograph revealed the morphology of the synthetic silver nanoparticles to be more or less spherical. Under SEM, the tested silver nanoparticles appear to form aggregates and individualized spherical particles with a mean particle size of around 20 nm (figure 1). At magnification of 50000x, it appears to be singlet segregated particles with completely spherical appearance, while at lower magnification of 35000x it appears to be more aggregated.

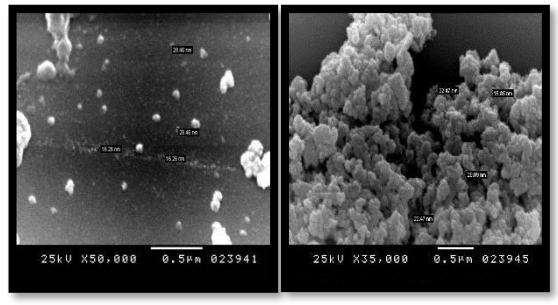

Figure 1: Scanning electron micrograph showing silver nanoparticles spheres with average size 20-22 nm. Panel (A) at a magnification of 50,000x and Panel (B) at a 35,000x.

3.2 Biodistribution and Accumulation of Silver Nanoparticles in Brain Cells

Using transmission electron microscope (TEM) specimen of different parts of brain cells, AgNPs appears to be distributed in the brain cells and

persisted mainly in lysosomes in rats treated with silver nanoparticles as shown in figure 2 when compared to control group (figure 2) which appeared to be free from silver nanoparticles. The acidic pH of lysosomes represents a good habitant for silver particles and an excellent co-factor for the release of silver ions [40]. This finding was in agreement with the study of Skalska *et al*., 2015 who found that nanoparticle structures located and localized in cellular lysosomes and between lamellae of myelin sheaths using TEM [41]. Using the same method of analysis, nanosized granules were detected in lysosomal cell compartment of AgNPs-treated astrocytic and neuronal cultures by Haase *et al*., 2012 [42].

Rats receiving 10 nm AgNPs chronically were found to accumulate AgNPs in lysosomes of endothelial cells [41]. On this basis, it is assumed that AgNPs influence the function of endothelial cells by increasing permeability of microvessels. Likely, existing in vitro data have identified perforations in the monolayer of rat brain microvessel endothelial cells exposed to AgNPs [43].

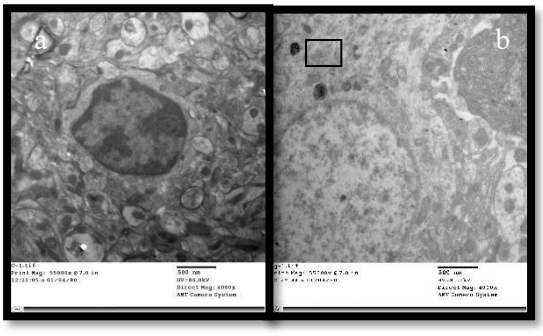

Figure 2: Transmission electron micrograph showing brain cells of control group (a) and brain cells from silver treated rats in which silver nanoparticles appear to be accumulated in lysosomes.

3.3 Effect of Different Doses of Silver Nanoparticle on Hematological Parameters of Male Rats

Significant decrease in TLC was seen only in group treated with the highest dose chronically. Groups treated with either single acute dose or low chronic dose showed a mild but not significant decrease in TLC compared to control group figure 3. A significant increase in TEC in all treated groups was observed in figure 3 when compared to control.

Significant decrease in hemoglobin concentration was also observed among all treated groups either with acute dose or chronically as shown in figure 3. There was no significant change in hematocrite concentration compared with control group.

A Significant decrease in MCV, MCH and MCHC was found in all treated groups compared to control group. This reduction is due to the reduction seen in hemoglobin concentration figure 3.

As shown in previous studies, the toxic implication of silver nanoparticles on hematological parameters is dose and rout dependent. In our present study, the increased number of RBC's with reduction in Hb, MCV, MCH and MCHC may be associated with degenerative effect of silver nanoparticles thus compensation of decreased oxygen-carrying capacity of Hb and RBCs by increasing the number of RBC [44, 45]. These adverse effects may be the degeneration of Hb and RBCs, destruction of hematopoietic tissue, and inhibition of aerobic glycolysis and the lack of enough energy for Hb synthesis [46, 47]. However, the reduction in WBC's was suggested to be due to suppressive effect of nanosilver on pluripotnt stem cells responsible for production of blood cells [21, 48, 49].

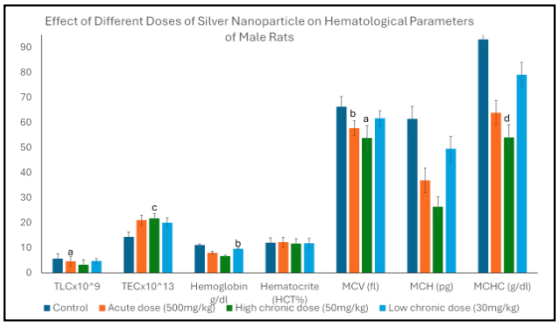

Figure 3: Dose-Dependent Hematological Effects of silver Nanoparticles. [a]Slightly significan difference, [b]Significant difference against control ($P < 0.05$), [c]Very significant difference against control ($P < 0.01$), [d]Extremely significant difference against control ($P < 0.001$).

3.4 Effect of Silver Nanoparticles on Antioxidant Enzymes

Significant increase in GST activity in groups treated with high chronic dose and acute dose compared with control group. While a non-significant increase was seen in rats treated with low chronic dose and figure 4, this increase in activity may be an indication of a defensive mechanism due to oxidative stress mechanism caused by silver ion itself. When comparing to control group, a significant increase in GPx activity was seen in all treated groups figure 4.

Significant decrease in total glutathione reduced was seen in acute dose and high chronic dose treated groups compared with control group, but low chronic dose shows mild but not significant reduction in GSH when compared with control figure 4. When compared with control group, there was a significant inhibition of liver catalase activity

in all treated groups. The inhibition was more pronounced in groups treated with chronic doses figure 4.

These results are similar to what Arora *et al.*, 2009 have assessed. The oxidative stress induced toxicity of silver NPs was detected by a depletion of glutathione reductase (2.5 folds) and a 2 fold increase in glutathione peroxidase. These results suggest oxidative damage to cells after exposure to AgNPs [24]. Oczkowski *et al.*, 2024 [9] also reported that after longer exposure period Ag-NPs cause an increase in GPx and GR activities and decrease in CAT activity. Both CAT and GPx participate in hydrogen peroxide (H_2O_2) removal which seems to be performed only by GPx in response to Ag-NPs; as GPx use glutathione as co-factor, the increase in GR activity is consistent with increase in glutathione recycling which is an essential mechanism to keep normal glutathione levels in cells and in consequence to keep cell homeostasis. Results indicate that, in *E. fetida*, CAT is activated in short exposure periods (4 days) although impaired for longer periods (28 days). This, together with GPx (that remains increased), are responding to an increase in H_2O_2 production, however not enough to prevent oxidative damage observed in increased levels of lipidperoxide levels [50]. The same was found by Choi *et al.*, 2010 who stated that CAT expression decreased 2.6- and 16.3-fold in zebrafish liver when compared to controls after treatment with AgNPs at 60 and 120 mg Ag/L, respectively [51]. Crago *et al.*, 2011 reported a significant increase in fat head minnow GST mRNA transcripts after exposure to silver nanoparticles. This increase in expression levels of GST which was observed could indicate the toxic effects and oxidative stress resulting from AgNPs toxicity [52].

Several studies on the expression of GPx gene have been conducted. In *C. riparius*, Nair *et al.*, 2012 reported GPx1 expression was up-regulated as a result of oxidative stress. [52, 53, 54] It has also been reported from that expression of GPx was induced due to oxidative stress caused by environmental stress conditions, such as metals and H_2O_2 [55].

Silver in its ionic form exhibits a high affinity for protein thiol groups and promotes their oxidation. Reduced glutathione (GSH) has also been shown to be a target of ionic silver which significantly depletes the pool of this major cellular antioxidant defense system. The influence of AgNPs on the level of SH groups has been confirmed in a myelin fraction isolated from brains of exposed adult rats [56]. Furthermore, exposure to low doses of small-diameter AgNPs (10 nm) significantly cause a decrease in the ratio of the reduced to the oxidized form of GSH in brain homogenates [41].

Hussain *et al.*, 2005 have observed GSH depletion in liver cells exposed to Ag (15, 100 nm) which is strongly correlated with increased ROS generation. It is possible that the loss of GSH may compromise cellular antioxidant defenses and lead to the accumulation of reactive oxygen species (ROS) [57].

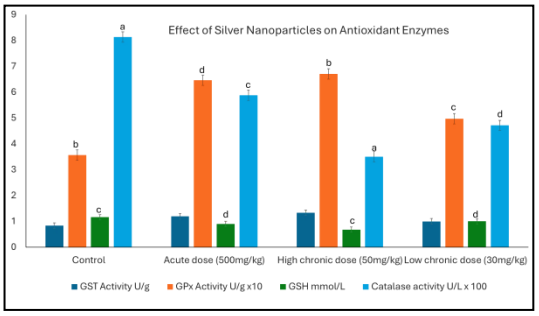

Figure 4: Dose-Dependent Effects of silver Nanoparticles on Antioxidants. [a]Slightly significan difference, [b]Significant difference against control ($P < 0.05$), [c]Very significant difference against control ($P < 0.01$), [d]Extremely significant difference against control ($P < 0.001$).

3.5 Effect of Different Doses of Silver Nanoparticle on Liver Enzymes

There is a significant decrease in AST, ALT and ALP in all treated groups comparing with control group. This inhibition may be an indication of hepatic cellular intoxication due to silver ions figure 5.

Maneewattanapinyo *et al.,* 2011 found that the treatment of rats with 100 mg/kg AgNPs decreased levels of AST and ALT enzyme significantly, whereas there were increases in AST levels in serum, kidney, and heart for the 14- and 21-day treatment groups. Treatment of rats with 1000 mg/kg and 5000 mg/kg AgNPs led to a significant decrease in ALT levels and a significant increase in AST levels for the 14- and 21-day treatment groups. In contrast, AST levels significantly decreased while ALT levels increased in rat serum treated with colloidal AgNPs for 7 days when compared with those treated for 21 days [58]. Kim *et al.*, 2009 on sub-chronic exposure of AgNPs to male and female rats over 90 days showed a significant decrease in the levels of serum AST and ALT. [20] Adewumi *et al.* 2014 recorded that on oral exposure of rats to AgNPs at various concentrations altered the serum and tissue levels of ALP relative to the control [59]. In serum, levels of ALP increased with increasing length of treatment administration. In contrast, non-significant reductions were recorded for tissue levels of ALP caused by AgNPs treatments. The rat serum and tissue levels of AST were inconsistently affected relative to the control. Conversely, there was significant reduction in the

levels of ALT in rat serum which was dose and duration dependent [60]. Many researches revealed that levels of AST, ALT and ALP in serum and tissue is a dose and duration dependent. When liver cells are damaged, plasma levels of AST, ALT and ALP increase above normal levels while the concentrations of these enzymes are diminished in liver cells itself. The amount of increase in plasma or decrease in hepatocytes is an indication of the degree of liver damage [61, 62].

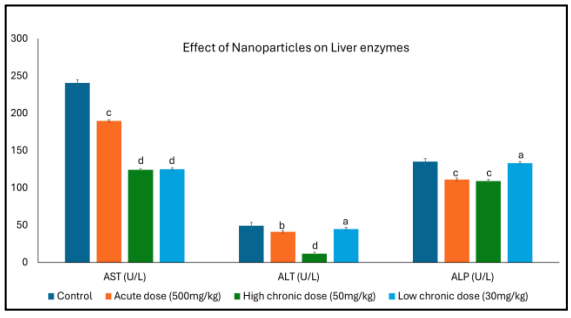

Figure 4: Dose-Dependent Effects of silver Nanoparticles on Liver Enzymes. [a]Slightly significan difference, [b]Significant difference against control ($P < 0.05$), [c]Very significant difference against control ($P < 0.01$), [d]Extremely significant difference against control ($P < 0.001$).

3.6 Effect of Silver Nanoparticles on Lipid Peroxidation

The extent of lipid peroxidation in the tissues is an indication of oxidation stress of the cell. Lipid peroxidation is defined as the deterioration of double bonds of unsaturated fatty acids by free radicals. Hepatic malondialdhyde was detected by Choi *et al*. 2010 to be significantly increased in zebrafish liver after treatment with AgNPs [51].

A significant increase in TBARS was found in all treated groups when compared to control group Table 1.

Table 1: Changes in Thiobarbituric acid reactive substances (TBARS nmol/ml) in male rats treated with different doses of silver nanoparticles**:**

Dose	TBARS concentration (nmol/ml)
Control	31.3 ± 1.3^{a}
Acute dose (500mg/kg)	38.8 ± 1.3^{b}
High chronic dose (50mg/kg)	40 ± 1.5^{c}
Low chronic dose (30mg/kg)	37.1 ± 1.4^{b}

[a]Slightly significan difference, [b]Significant difference against control ($P < 0.05$), [c]Very significant difference against control ($P < 0.01$), [d]Extremely significant difference against control ($P < 0.001$).

3.7 Effect of Silver Nanoparticles on Brain of Male Rats

A significant reduction in total protein content of brain was seen in rats treated with acute dose and high chronic dose of silver nanoparticles when compared to control group. There was a mild reduction in total protein in low dose group of silver NPs, figure 5.

Treatment of rats with AgNPs caused elevation ($P< 0.05$) in total protein levels in rat liver. In contrast, the levels of total protein were reduced in rat serum, kidney, brain and heart for groups treated with AgNPs.

Compared to control, there was a significant decrease in AchE. Activity in rats treated with low dose and single acute dose. While, in contrast, there was a significant increase in rats treated with the high dose of silver NPs figure 5. It appears that variation in AchE activity is a dose and duration dependent.

Wang *et al*., 2009 studied the toxic effects of nanoparticles on AChE activity in vitro. Different classes of nanoparticles, including metals, oxides, and carbon nanotubes showed high affinity for AChE. Cu, Cu–C multiwalled carbon nanotubes, and single walled carbon nanotubes showed a dose related inhibition of AChE activity with. The inhibition by nanoparticles was primarily caused by adsorption or interaction with the enzyme [46].

The potential of some metallic ions, such as lead, copper, cadmium and mercury to depress the activity of AChE in vitro and in vivo conditions has been demonstrated in several studies on humans and animals [47].

The potential effect of lead on erythrocyte AChE activity during occupational exposure to this metal and suggested that AChE activity could be considered as a biomarker of lead-induced neurotoxicity in occupational exposed subjects. [22]

In the present results of our study, the inhibition of AChE enzyme in both acute dose and lower chronic dose is similar to what was found in previous studies done on different types of nanoparticles. [22]. While the increase in AChE activity which was seen in the higher chronic dose is similar to the explanation done by Melo *et al.*, 2003 that the increased ROS as a result of high levels of lipid peroxidation decreased cell membrane order and ultimately led to the exposure of more active sites of the AChE [49]. As a consequence, AChE activity was increased which likely happened with high chronic dose of AgNPs due to higher peroxidation level and thus higher ROS production [49].

A significant inhibition of Na^{+}/K^{+} ATPase activity was seen in chronically treated groups when

compared to control group. While, there was no significant change in Na^+/K^+ ATPase activity in acute dose treated group figure 5.

Current results are in agreement with previous studies conducted to assess silver nanoparticles toxicity. It was reported that AgNPs induced alterations of mitochondrial membrane permeability and uncoupling of the oxidative phosphorylation system in cells [50].

Asha Rani *et al.,* 2008 suggested that AgNPs led to Structural and functional damage of the mitochondria that could result in metabolic arrest, followed by a decrease in ATP yield. Deposition of Ag-np in mitochondria can alter normal functioning of mitochondria by disrupting the electron transport chain, ultimately resulting in ROS and low ATP yield [63].

Wood *et al.,* 1999 reported Ag^+ basically affects the inhibition of Na^+, K^+ ATPase activity through a noncompetitive inhibition of active gill transport of Na^+ and Cl^-, increasing the intracellular acidity and partially inhibiting carbonic anhydrase by hydration [64].

Mohammadbakir *et al.,* 2016 found that the consequences of Ag toxicity can be found in the inhibition of thiol-containing proteins. Ag toxicity depletes the levels of intracellular ATP by the binding of Ag^+ to sulfhydryl (SH) groups of Na^+/K^+ ATPase [65].

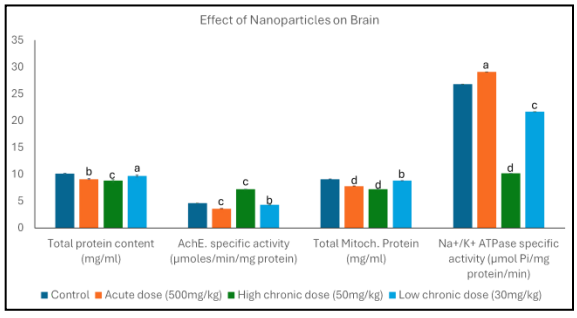

Figure 5: Dose-Dependent Effects of silver Nanoparticles on Brain. [a]Slightly significan difference, [b]Significant difference against control ($P < 0.05$), [c]Very significant difference against control ($P < 0.01$), [d]Extremely significant difference against control ($P < 0.001$).

3.8 Effect of Silver nanoparticles on the Expression Level of genes

A significant increase in the level of iNOS expression in all treated animal groups when compared with the control group (6.63 fold in acute dose group, 4.46 fold in high chronic dose group and 4.05 fold in low chronic dose group). (figure 6).

The gene expression levels of iNOS was found to be upregulated and this observation was thought to be linked with with Aβ accumulation in brain cells which disrupts multiple signal transduction systems [66]. Previous studies indicated that AgNPs caused Aβ amyloid plaque deposition in mouse neuron cells. The ability of insoluble peptides of Aβ amyloid has been considered more rapidly aggregation and more neurotoxicity in Alzheimer disease progression [67]. Huang *et al*., 2015 reported that AgNPs exposure can induce Aβ peptides aggregation in neural cells. Moreover, the gene expression and protein level of Aβ amyloid generation and deposition relevant to AD progression have been explored after AgNPs exposure [68]. Sharma *et al*., 2013 in a study on the toxicity of different types of nanoparticles, Ag NPs irrespective of their sizes was found to induce greater nNOS expression in neurons followed by Cu and Al NPs. The molecular mechanisms of silver NPs toxicity was examined using expression of neuronal NOS in the cortex of different age group of rats after NPs administration. The results show the smallest size of NPs from Cu, Ag, or Al induces profound up-regulation of nNOS expression in the cerebral cortex of the animals. Smaller size of NPs induces higher number of NOS positive neurons in the cortex compared to larger sizes of NPs [69].

Significant increase in expression level of TH was seen in all treated groups when compared with control group figure 6. The biosynthesis of dopamine and other catecholamines can be limited by the action of enzyme tyrosine hydroxylase (TH) therefore; levels of TH expression can be an indication of physiological changes [70]. In female rats, it Hadrup *et al*., 2012 has reported that 14 nm Ag-NPs with different doses increased the dopamine concentration in the brain following 28 days of oral administration [71]. At the same study, the dopamine concentration in the brain decreased by Ag-NPs following a 14-day exposure. Seyed *et al*., 2016 has found that exposure of rat to AgNPs during the pregnancy caused a dose-dependent up-regulation of TH in the brain of offspring at various age after birth in relation to control animals. TH mRNA expression was increased in an age-dependent manner in exposed offspring. The highest expression was reported with the highest dose and increasingly with time [32]. Hussain *et al.*, 2006 have shown that Ag-NPs (15 nm) moderately decrease dopamine content in a dopaminergic neuronal cell line (PC12) after 24 hours of exposur [72]. On the same track, Wang *et al*., studied the toxic action of Cu, Mn, and Ag nanoparticles on 11 genes expression related to dopamine concentration in neuronal cells PC12. It was found that these NPs induced a lower production of dopamine after 24 hours of exposure [50].

These diverging results suggested that an early decrease in dopamine level induced by Ag-NPs is

followed by a compensatory increase by increased exposure time. The initial low levels of dopamine could be explained by an increase in apoptosis of dopaminergic neurons. Exposure of tyrosine hydroxylase (TH), the rate-limiting enzyme in dopamine synthesis, to peroxynitrite, an oxidative stress product, results in nitration of tyrosine residues and modification of cysteines leading to decreased catalytic activity [73].

Taken together, these data support the possibility that the effects of silver nanoparticles on dopamine brain concentrations can vary depending on either the length or dose of the exposure [74].

Effect of silver nanoparticles on % Expression of monocyte chemoatractant protein1 (MCP-1) gene in rats was tested on SNPs treated animals as shown in figure 6. It was found that, the expression levels of MCP-1 was significantly increased in brain tissues of all treated animals as compared to the control group. Madrigal *et al.*, in 2010 demonstrated that animals exposed to certain types of stress produced significant amount of MCP-1 and this upregulation in the expression level could be through the inhibitory activity of glucocorticoids during the stress reaction. Moreover, when the production of glucocorticoids by stressed rats is blocked by the selective inhibitor, a large increase in the concentration of MCP-1 was observed in the cortex [75]. Ciechanowska *et al.*, 2024 found the AgNPs treated liver cells have the up-regulated gene expression of CXCL13 to induce apoptosis and inflammation. Moreover, chemokine C–C motif ligand (CCL) 2 can activate resident microglias in the brain to recruit peripheral macrophages and increase chemokine family CCL2 gene expression [76]. Effect of silver nanoparticles on % Expression of vesicular monoamine transporter (VMAT) gene in rats showed Significant increase in expression level of VMAT was seen in all treated groups when compared with control group figure 6. From previous studies it was found that, VMAT 2 concentration is directly proportional to the concentration of intracellular dopamine. As Hadrup *et al.*, 2012 and Tabatabaie *et al.*, 2016 found that DA concentration increased after AgNPs exposure [71, 77].

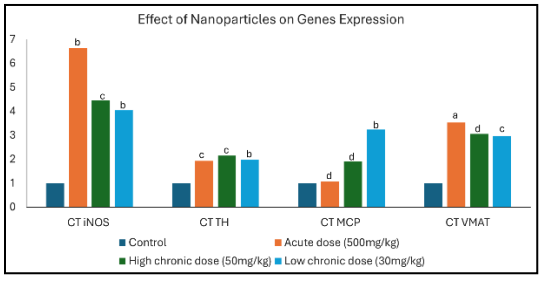

Figure 6: The effect (Log2, fold change) of Silver Nanoparticles on iNOS, tyrosine hydroxylase (TH), monocyte chemoatractant protein1 (MCP-1)and vesicular monoamine transporter (VMAT) transcription levels using Real time PCR. [a]Slightly significan difference, [b]Significant difference against control ($P < 0.05$), [c]Very significant difference against control ($P < 0.01$), [d]Extremely significant difference against control ($P < 0.001$).

4. Conclusion

It has become popular to incorporate silver in its nanoform into products such as cosmetics, textiles, food boxes, sprays, wound dressings; etc. Silver nanoparticles have a wide usage in medicine as antibacterial, antiviral, antiproliferative, sensory and imaging agent and in tissue engineering.

Due to physical and chemical properties of silver as metal nanoparticles, it has so many adverse reactions and toxicological issues that should be considered in mind. Silver NPs can translocate and accumulate in vital organs as brain, lung and liver. This may result in inflammation and stress in these organs leading to serious diseases. The main toxicological concern of silver nanoparticles is that it has the ability to cause oxidative stress in body organs which is resulted due to the silver ion itself.

Acute and chronic toxicity of silver nanoparticles was determined in wistar male rats treated intraperitoneal with different doses of silver nanoparticles for three weeks. Rats with average weight of 150 g were divided into four groups. The first group served as a control group and treated with normal saline. Groups 2, 3 and 4 were treated with acute dose 500mg/kg/body weight, chronic dose 50mg/kg/body weight and chronic dose 30mg/kg/body weight respectively of silver nanoparticles.

Blood samples were collected for hematological testing and liver and brain was isolated and kept at -80ºC until used for biochemical and molecular analysis. Brain sample was prepared for examination of silver nanoparticles accumulation in brain cells using TEM.

Hematological parameters like total leukocyte count, total erythrocyte count, hemoglobin, hematocrite, MCV, MCH and MCHC were measured. Biochemical analysis in liver included a set of biochemical tests like liver function tests, GST, GPx, CAT, GSH and level of TBARS. Biochemical analysis in brain included measurement of AChE activity and Na^+/K^+ ATPase activity.

5. References

1. Das KP. Nanoparticles and convergence of artificial intelligence for targeted drug delivery for cancer therapy: Current progress and challenges. Front Med Technol. 2023;4:1067144. https://doi.org/10.3389/fmedt.2022.1067144
2. Fröhlich E. Models for oral uptake of nanoparticles in consumer products. Toxicology. 2012;291:1-11. https://doi.org/10.1016/j.tox.2011.11.004

3. Fernandez CC, Sokolonski AR, Fonseca MS, Stanisic D, Araújo DB, Azevedo V, et al. Applications of silver nanoparticles in dentistry: Advances and technological innovation. Int J Mol Sci. 2021;22(5):2485. https://doi.org/10.3390/ijms22052485
4. Bachler G, von Goetz N, Hungerbühler K. A physiologically based pharmacokinetic model for ionic silver and silver nanoparticles. Int J Nanomedicine. 2013;8:3365-82. https://doi.org/10.2147/IJN.S46624
5. Karade VC, Patil RB, Parit SB, Kim JH, Chougale AD, Dawkar VV. Insights into shape-based silver nanoparticles: A weapon to cope with pathogenic attacks. ACS Sustain Chem Eng. 2021;9(37):12476-507. https://doi.org/10.1021/acssuschemeng.1c03797
6. Salem W, Zingl DR, Schratter G, Prassl R, Goessler W, Reidl J, et al. Antibacterial activity of silver and zinc nanoparticles against Vibrio cholerae and enterotoxic Escherichia coli. Int J Med Microbiol. 2015;305:85-95. https://doi.org/10.1016/j.ijmm.2014.11.005
7. More PR, Pandit S, Filippis AD, Franci G, Mijakovic I, Galdiero M. Silver nanoparticles: Bactericidal and mechanistic approach against drug-resistant pathogens. Microorganisms. 2023;11(2):369. https://doi.org/10.3390/microorganisms11020369
8. Takáč P, Michalková R, Čižmáriková M, Bedlovičová Z, Balážová Ľ, Takáčová G. The role of silver nanoparticles in the diagnosis and treatment of cancer: Are there any perspectives for the future? Life. 2023;13(2):466. https://doi.org/10.3390/life13020466
9. Oczkowski M, Dziendzikowska K, Gromadzka-Ostrowska J, Kruszewski M, Grzelak A. Intragastric exposure of rats to silver nanoparticles modulates the redox balance and expression of steroid receptors in testes. Food Chem Toxicol. 2024;191:114841. https://doi.org/10.1016/j.fct.2024.114841
10. Lee JH, Kim YS, Song KS, Ryu HR, Sung JH, Park JD, et al. Biopersistence of silver nanoparticles in tissues from Sprague-Dawley rats. Part Fibre Toxicol. 2013;10(36):1-17. https://doi.org/10.1186/1743-8977-10-36
11. Ferdous Z, Nemmar A. Health impact of silver nanoparticles: A review of the biodistribution and toxicity following various routes of exposure. Int J Mol Sci. 2020;21(7):2375. https://doi.org/10.3390/ijms21072375
12. Sharma HS, Ali SF, Hussain SM, Schlager JJ, Sharma A. Influence of engineered nanoparticles from metals on the blood-brain barrier permeability, cerebral blood flow, brain edema, and neurotoxicity. J Nanosci Nanotechnol. 2009;9:5055-72. https://doi.org/10.1166/jnn.2009.GR09
13. Salama B, Alzahrani KJ, Alghamdi KS, Al-Amer O, Hassan KE, Elhefny MA, et al. Silver nanoparticles enhance oxidative stress, inflammation, and apoptosis in liver and kidney tissues: Potential protective role of thymoquinone. Biol Trace Elem Res. 2023;201(6):2942-54. https://doi.org/10.1007/s12011-022-03399-w
14. Lankveld DP, Oomen AG, Krystek P, Neigh A, Troost-de Jong A, Noorlander CW, et al. The kinetics of the tissue distribution of silver nanoparticles of different sizes. Biomaterials. 2010;32:100-9. https://doi.org/10.1016/j.biomaterials.2010.07.045
15. Sharma HS, Schlager JJ, Ali SF, Sharma A. Influence of nanoparticles on blood-brain barrier permeability and brain edema formation in rats. Acta Neurochir Suppl. 2010;106:359-64. https://doi.org/10.1007/978-3-211-98811-4_65
16. Krishnan V, Mitragotri S. Nanoparticles for topical drug delivery: Potential for skin cancer treatment. Adv Drug Deliv Rev. 2020;153:87-108. https://doi.org/10.1016/j.addr.2020.05.011
17. Samberg ME, Oldenburg SJ, Monteiro-Riviere NA. Evaluation of silver nanoparticle toxicity in skin in vivo and keratinocytes in vitro. Environ Health Perspect. 2010;118(3):407-13. https://doi.org/10.1289/ehp.0901398
18. Bin-Jumah M, Al-Abdan M, Albasher G, Alarifi S. Effects of green silver nanoparticles on apoptosis and oxidative stress in normal and cancerous human hepatic cells in vitro. Int J Nanomedicine. 2020;15:1537-48. https://doi.org/10.2147/IJN.S239861
19. Min Y, Suminda GG, Heo Y, Kim M, Ghosh M, Son YO. Metal-based nanoparticles and their relevant consequences on cytotoxicity cascade and induced oxidative stress. Antioxidants. 2023;12(3):703. https://doi.org/10.3390/antiox12030703
20. Kim S, Choi J, Chung KH, Park K, Yi J, Ryu DY. Oxidative stress-dependent toxicity of silver nanoparticles in human hepatoma cells. Toxicol In Vitro. 2009;23(6):1076-84. https://doi.org/10.1016/j.tiv.2009.06.001
21. Costa CS, Rambo JG, Daufenbach JF, Gonçalves CL, Rezin GT, Streck EL, et al. In vitro effects of silver nanoparticles on the mitochondrial respiratory chain. Mol Cell Biochem. 2010;342(1-2):141-7. https://doi.org/10.1007/s11010-010-0467-9
22. Yang H, Niu S, Guo M, Xue Y. Molecular mechanisms of silver nanoparticle-induced neurotoxic injury and new perspectives for its neurotoxicity studies: A critical review. Environ Pollut. 2024;124934. https://doi.org/10.1016/j.envpol.2024.124934
23. Yildirimer L, Thanh NT, Loizidou M, Seifalian AM. Toxicological considerations of clinically applicable nanoparticles. Nano Today. 2011;6(5):585-607. https://doi.org/10.1016/j.nantod.2011.10.001
24. Arora S, Jain J, Rajwade JM, Paknikar KM. Interactions of silver nanoparticles with biological systems. Toxicol Lett. 2008;179(2):93-100. https://doi.org/10.1016/j.toxlet.2008.04.009
25. Lowry OH, Rosebrough NJ, Farr AL, Randall RJ. Protein measurement with the folin phenol reagent. J Biol Chem. 1951;193(1):265-75. https://doi.org/10.1016/S0021-9258(19)52451-6
26. Wintrobe MM. Blood of normal young women residing in a subtropical climate: red cells, hemoglobin, volume of packed red cells, color index, volume index, and saturation index. Arch Intern Med. 1930;45(2):287-301.

https://doi.org/10.1001/archinte.1930.00140080129010
27. Reitman S, Frankel S. Determination of serum glutamic oxaloacetic and glutamic pyruvic acid transaminases. Am J Clin Pathol. 1957;28(1):56-63. https://doi.org/10.1093/ajcp/28.1.56
28. Belfield A, Goldberg DM. Revised assay for serum phenyl phosphatase activity using 4-amino-antipyrine. Enzyme. 1971;12(5):561-73. https://doi.org/10.1159/000459586
29. Ellman GI, Courtney KD, Andres V Jr, Featherstone RM. A new and rapid colorimetric determination of acetylcholinesterase activity. Biochem Pharmacol. 1961;7:88-95. https://doi.org/10.1016/0006-2952(61)90145-9
30. Koch RB. Chlorinated hydrocarbon insecticides: inhibition of rabbit brain ATPase activities. J Neurochem. 1969;16(2):269-71. https://doi.org/10.1111/j.1471-4159.1969.tb05944.x
31. Taussky HH, Shorr E. A microcolorimetric method for the determination of inorganic phosphorus. J Biol Chem. 1953;202(2):675-85. https://doi.org/10.1016/S0021-9258(18)66180-0
32. Habig WH, Pabst MJ, Jacoby WB. Glutathione S-transferase: the first enzymatic step in mercapturic acid formation. J Biol Chem. 1974;249(22):7130-9. https://doi.org/10.1016/S0021-9258(19)42083-8
33. Beutler E, Duron O, Kelly BM. Improved method for the determination of blood glutathione. J Lab Clin Med. 1963;61:882-8.
34. Aebi H. Catalase in vitro. Methods Enzymol. 1984;105:121-6. https://doi.org/10.1016/S0076-6879(84)05016-3
35. Fossati P, Prencipe L, Berti G. Use of 3,5-dichloro-2-hydroxybenzenesulfonic acid/4-aminophenazone chromogenic system in direct enzyme assay of uric acid in serum and urine. Clin Chem. 1980;26(2):227-31. https://doi.org/10.1093/clinchem/26.2.227
36. Paglia DE, Valentine WN. Studies on the quantitative and qualitative characterization of erythrocyte glutathione peroxidase. J Lab Clin Med. 1967;70(1):158-69.
37. Tappel AL, Zalkin H. Inhibition of lipid peroxidation in mitochondria by vitamin E. Arch Biochem Biophys. 1959;80(2):333-6. https://doi.org/10.1016/0003-9861(59)90259-0
38. Sambrook J, Fritsch EF, Maniatis T. Molecular cloning: a laboratory manual. 2nd ed. Cold Spring Harbor, NY: Cold Spring Harbor Laboratory Press; 1989.
39. Yang G, Erdman DE, Kodani M, Kools J, Bowen MD, Fields BS. Comparison of commercial systems for extraction of nucleic acids from DNA/RNA respiratory pathogens. Journal of virological methods. 2011 Jan 1;171(1):195-9.
40. Setyawati MI, Yuan X, Xie J, Leong DT. The influence of lysosomal stability of silver nanomaterials on their toxicity to human cells. Biomaterials. 2014;35(23):6707-15. https://doi.org/10.1016/j.biomaterials.2014.05.007
41. Skalska J, Frontczak-Baniewicz M, Struzynska L. Synaptic degeneration in rat brain after prolonged oral exposure to silver nanoparticles. Neurotoxicology. 2015;46:145-54. https://doi.org/10.1016/j.neuro.2014.11.002
42. Haase A, Rott S, Mantion A, Graf P, Plendl J, Thunemann AF, et al. Effects of silver nanoparticles on primary mixed neural cell cultures: uptake, oxidative stress, and acute calcium responses. Toxicol Sci. 2012;126(2):457-68. https://doi.org/10.1093/toxsci/kfs003
43. Suthar JK, Vaidya A, Ravindran S. Toxic implications of silver nanoparticles on the central nervous system: A systematic literature review. J Appl Toxicol. 2023;43(1):4-21. https://doi.org/10.1002/jat.4317
44. Olugbodi JO, David O, Oketa EN, Lawal B, Okoli BJ, Mtunzi F. Silver nanoparticles stimulate spermatogenesis impairments and hematological alterations in testis and epididymis of male rats. Molecules. 2020;25(5):1063. https://doi.org/10.3390/molecules25051063
45. Atamanalp M, Kocaman EM, Ucar A, Şişman T, Turkez H. The alterations in the hematological parameters of rainbow trout (Oncorhynchus mykiss) exposed to cobalt chloride. Kafkas Univ Vet Fak Derg. 2011;17:73-6.
46. Wang Z, Zhang J, Li F, Gao D, Xing B. Adsorption and inhibition of acetylcholinesterase by different nanoparticles. Chemosphere. 2009;77(1):67-73. https://doi.org/10.1016/j.chemosphere.2009.05.015
47. Egba SI, Famurewa AC, Omoruyi LE. Buchholzia coriacea seed extract attenuates mercury-induced cerebral and cerebellar oxidative neurotoxicity via NO signaling and suppression of oxidative stress, adenosine deaminase, and acetylcholinesterase activities in rats. Avicenna J Phytomed. 2022;12(1):42-55.
48. Nabi M, Tabassum N. Role of environmental toxicants in neurodegenerative disorders. Front Toxicol. 2022;4:837579. https://doi.org/10.3389/ftox.2022.837579
49. Melo JB, Agostinho P, Oliveira CR. Involvement of oxidative stress in the enhancement of acetylcholinesterase activity induced by amyloid beta-peptide. Neurosci Res. 2003;45(1):117-27. https://doi.org/10.1016/S0168-0102(02)00201-8
50. Wang L, Mello DF, Zucker RM, Rivera NA, Rogers NM, Geitner NK, et al. Lack of detectable direct effects of silver and silver nanoparticles on mitochondria in mouse hepatocytes. Environ Sci Technol. 2021;55(16):11166-75. https://doi.org/10.1021/acs.est.1c02295
51. Choi JE, Kim S, Ahn JH, Youn P, Kang JS, Park K, et al. Induction of oxidative stress and apoptosis by silver nanoparticles in the liver of adult zebrafish. Aquat Toxicol. 2010;100(2):151-9. https://doi.org/10.1016/j.aquatox.2009.12.012
52. Crago J, Corsi SR, Weber D, Bannerman R, Klaper R. Linking biomarkers to reproductive success of caged fathead minnows in streams with increasing urbanization. Chemosphere. 2011;82(11):1669-74. https://doi.org/10.1016/j.chemosphere.2010.11.011
53. Nair PM, Choi J. Characterization and transcriptional regulation of thioredoxin reductase 1 on exposure to oxidative stress-inducing environmental pollutants in Chironomus riparius. Comp Biochem Physiol B Biochem Mol Biol. 2012;161(2):134-9.
54. Chen F, Zhao CY, Guan JF, Liu XC, Li XF, Xie DZ,

et al. High-carbohydrate diet alleviates oxidative stress, inflammation, and apoptosis of Megalobrama amblycephala following dietary exposure to silver nanoparticles. Antioxidants. 2021;10(9):1343. https://doi.org/10.3390/antiox10091343
55. Jomova K, Raptova R, Alomar SY, Alwasel SH, Nepovimova E, Kuca K, et al. Reactive oxygen species, toxicity, oxidative stress, and antioxidants: Chronic diseases and aging. Arch Toxicol. 2023;97(10):2499-574.
56. Dąbrowska-Bouta B, Sulkowski G, Zięba M, Orzelska J, Strużyńska L. Oxidative stress in myelin of the rat brain exposed to silver nanoparticles. Folia Neuropathol. 2015;53(4):281-9.
57. Hussain SM, Hess KL, Gearhart JM, Geiss KT, Schlager JJ. In vitro toxicity of nanoparticles in BRL 3A rat liver cells. Toxicol In Vitro. 2005;19(7):975-83.
58. Maneewattanapinyo P, Banlunara W, Thammacharoen C, Ekgasit S, Kaewamatawong T. An evaluation of acute toxicity of colloidal silver nanoparticles. J Vet Med Sci. 2011;73(11):1417-23. https://doi.org/10.1292/jvms.11-0038
59. Adewumi OS, Adenuga IO. Biochemical evaluation of silver nanoparticles in Wistar rats. Int Schol Res Notices. 2014;2014:196091. https://doi.org/10.1155/2014/196091
60. Omara MO, Sarhan RM. Effects of intraperitoneally injected silver nanoparticles on histological structures and blood parameters in the albino rat. Int J Nanomedicine. 2014;9:1505-17. https://doi.org/10.2147/IJN.S56729
61. Dambach DM, Andrews BA, Moulin F. New technologies and screening strategies for hepatotoxicity: Use of in vitro models. Toxicol Pathol. 2005;33(1):17-26. https://doi.org/10.1080/01926230590522284
62. Metwally MD, Etorki MA. Acute effect of nanosilver on liver function and tissue in rats after intraperitoneal injection. J Biol Sci. 2014;14(3):213-9. https://doi.org/10.3923/jbs.2014.213.219
63. AshaRani PV, Low Kah Mun G, Prakash Hande M, Valiyaveettil S. Cytotoxicity and genotoxicity of silver nanoparticles in human cells. ACS Nano. 2008;3(2):279-90. https://doi.org/10.1021/nn800596w
64. Wood CM, Playle RC, Hogstrand C. Physiology and modeling of mechanisms of silver uptake and toxicity in fish. Environ Toxicol Chem. 1999;18(1):71-83. https://doi.org/10.1002/etc.5620180110
65. Mohammadbakir S. Impacts of waterborne copper and silver on the early life stage (ELS) of zebrafish (Danio rerio): physiological, biochemical, and molecular responses [Doctoral dissertation]. Plymouth: Plymouth University; 2020.
66. Anwar MM. Oxidative stress: A direct bridge to central nervous system homeostatic dysfunction and Alzheimer's disease. Cell Biochem Funct. 2022;40(1):17-27. https://doi.org/10.1002/cbf.3673
67. Jeremic D, Jiménez-Díaz L, Navarro-López JD. Past, present, and future of therapeutic strategies against amyloid-β peptides in Alzheimer's disease: A systematic review. Ageing Res Rev. 2021;72:101496. https://doi.org/10.1016/j.arr.2021.101496
68. Huang CL, Lin IL, Lin HC, Wang CF, Huang YJ, Chuang CY. Silver nanoparticles affect gene expression of inflammatory and neurodegenerative responses in mouse brain neural cells. Environ Res. 2015;136:253-63. https://doi.org/10.1016/j.envres.2014.11.006
69. Sharma AR, Fornari MF, Patnaik R, Sharma HS. Size- and age-dependent neurotoxicity of engineered metal nanoparticles in rats. Mol Neurobiol. 2013;48:386-96. https://doi.org/10.1007/s12035-013-8500-0
70. Gonzalez-Lopez E, Vrana KE. Dopamine beta-hydroxylase and its genetic variants in human health and disease. J Neurochem. 2020;152(2):157-81. https://doi.org/10.1111/jnc.14893
71. Hadrup N, Loeschner K, Mortensen A, Sharma AK, Qvortrup K, Larsen EH, et al. Neurotoxic effects of nanoparticulate and ionic silver in vivo and in vitro. Neurotoxicology. 2012;33(3):416-23. https://doi.org/10.1016/j.neuro.2012.04.008
72. Hussain SM, Schrand AM, Duhart HM, Ali SF, Schlager JJ. Interaction of manganese nanoparticles with PC-12 cells induces dopamine depletion. Toxicol Sci. 2006;92(2):456-63. https://doi.org/10.1093/toxsci/kfl020
73. MohanKumar SM, Murugan A, Palaniyappan A, MohanKumar PS. Role of cytokines and reactive oxygen species in brain aging. Mech Ageing Dev. 2023;111855. https://doi.org/10.1016/j.mad.2023.111855
74. Tareq M, Khadrawy YA, Rageh MM, Mohammed HS. Dose-dependent biological toxicity of green-synthesized silver nanoparticles in rat brains. Sci Rep. 2022;12(1):22642. https://doi.org/10.1038/s41598-022-27171-1
75. Madrigal JL, Garcia-Bueno B, Hinojosa AE, Polak P, Feinstein DL, Leza JC. Regulation of MCP-1 production in the brain by stress and noradrenaline-modulating drugs. J Neurochem. 2010;113:543-51. https://doi.org/10.1111/j.1471-4159.2010.06623.x
76. Ciechanowska A, Mika J. CC chemokine family members' modulation as a novel approach for treating central and peripheral nervous system injury. Int J Mol Sci. 2024;25(7):3788. https://doi.org/10.3390/ijms25073788
77. Tabatabaie SRF, Bakhtiari NM, Tabandeh MR. Silver nanoparticle exposure in pregnant rats increases gene expression of tyrosine hydroxylase and monoamine oxidase in offspring brains. Drug Chem Toxicol. 2016;39(4):465-72.

Timeline of Publication
Received Date: 31 August 2024
Revised Date: 11 September 2024
Accepted Date: 16 September 2024
Published Date: 1 October 2024